JOURNAL OF NEUROTRAUMA 30:1812–1823 (November 1, 2013)

DOI: 10.1089/neu.2013.2993

Substance P as a Mediator of Neurogenic Inflammation after Balloon Compression Induced Spinal Cord Injury

Anna V. Leonard, Emma Thornton, and Robert Vink

Abstract

Although clinical spinal cord injury (SCI) occurs within a closed environment, most experimental models of SCI create an open injury. Such an open environment precludes the measurement of intrathecal pressure (ITP), whose increase after SCI has been linked to the development of greater tissue damage and functional deficits. Raised ITP may be potentiated by edema, which we have recently shown to be associated with substance P (SP) induced neurogenic inflammation in both traumatic brain injury and stroke. The present study investigates whether SP plays a similar role as a mediator of neurogenic inflammation after SCI. A closed balloon compression injury was induced at T10 in New Zealand white rabbits. Animals were thereafter assessed for blood spinal cord barrier (BSCB) permeability, edema, ITP, histological outcome, and functional outcome from 5 h to 2 weeks post-SCI. The balloon compression model produced significant increases in BSCB permeability, edema, and ITP along with significant functional deficits that persisted for 2 weeks. Histological assessment demonstrated decreased SP immunoreactivity in the injured spinal cord while NK1 receptor immunoreactivity initially increased before returning to sham levels. In addition, aquaporin 4 immunoreactivity increased early post-SCI, implicating this water channel in the development of edema after SCI. The changes described in the present study support a role for SP as a mediator of neurogenic inflammation after SCI.

Key words: blood spinal cord barrier; edema; neurogenic inflammation; spinal cord injury; substance P

Introduction

Spinal cord injury (SCI) is an unexpected event that is both devastating and debilitating, commonly resulting in permanent physical disability. To date, therapies have limited efficacy in preventing or attenuating the resultant functional deficits. To develop more effective therapies, it is essential that experimental models of SCI replicate the primary injury mechanisms that occur after human SCI—namely, an initial impact and persisting compression—and then to characterize the subsequent development of the secondary injury process. Many commonly used experimental models of SCI involve open injury models, in which a laminectomy is performed and the injury induced at the open site. Such an environment contrasts to the closed nature of most injuries experienced in the clinical environment and ignores the effects of persistent spinal cord compression on the secondary injury process and resultant functional outcome.

Edema development is an important secondary injury factor after traumatic SCI and has been well characterized both within the injury epicenter[1–6] and in the adjacent segments where a delayed spread of edema has been demonstrated.[7,8] Such edema may be both vasogenic and cytotoxic in nature; however, it has been hypothesized that the initial edema is predominantly vasogenic in nature given that blood-spinal cord-barrier (BSCB) disruption is also present.[1,2,9–11] Increased edema represents an important secondary injury process, because it may lead to raised intrathecal pressure (ITP).[12] Such an increase in ITP can only occur in a closed environment.

While a number of factors have been implicated in the development of edema after central nervous system (CNS) injury, we have recently shown that neurogenic inflammation plays an integral role.[13–19] Neurogenic inflammation is a response of perivascular, unmyelinated afferent nerve fibers to injury or infection and is typically characterized by vasodilation, protein extravasation, and edema.[13,14] The vascular response is facilitated by the release of neuropeptides such as substance P (SP) and calcitonin gene related peptide. SP is known to preferentially bind to the tachykinin NK1 receptor, activation of which results in increased barrier permeability and edema development.[14] Increased SP immunoreactivity has been associated with increased blood–brain barrier (BBB) permeability and edema development after both traumatic brain injury (TBI)[13,17] and stroke,[16] while antagonism of the NK1 receptor has been shown to reduce BBB permeability and edema, and improve functional outcome.[13,17,20] Whether substance P plays a similar role as a mediator of neurogenic inflammation after traumatic SCI has not yet been investigated.

The School of Medical Sciences, Level 4, Medical School South, The University of Adelaide, Adelaide, South Australia, Australia.

Accordingly, the current study uses a balloon compression model of SCI to characterize changes in SP immunoreactivity, BSCB permeability, edema, ITP, histological outcome, and functional outcome from 5 h to 2 weeks post-SCI. We have used the balloon compression model of SCI because of its closed nature and replication of key primary injury mechanisms such as an initial impact (rapid inflation of the balloon) and continued compression. Further, since its original conception by Tarlov and associates,[21,22] the balloon compression model has been shown to be consistent and reproducible, with many studies demonstrating a correlation between the severity of injury and functional deficits.[23]

Methods

All experimental protocols were conducted according to the guidelines established by the National Health and Medical Research Council and were approved by the animal ethics committees of the University of Adelaide and the Institute of Medical and Veterinary Sciences.

Balloon compression model of SCI

New Zealand white rabbits ($n = 88$) underwent a balloon compression SCI as described previously.[24,25] Briefly, during the 12-h day cycle, animals were removed from their home cages and anesthetized via a subcutaneous injection of a ketamine (2.5 mg/kg) and medetomidine HCl (0.25 mg/kg) mixture. Once a surgical level of anesthesia was achieved, the animal was placed onto a thermostatically controlled heating pad in the prone position. Initially, the dorsal surface of the animal's back was shaved and a midline incision of approximately 10 cm in length was made along the spinous processors (approximately T11–L2). Paraspinal muscles were retracted, and a laminectomy was performed. A balloon catheter (ApexTM MonorailTM 4 mm × 8 mm, Boston Scientific) was then inserted epidurally, within the vertebral canal, and advanced approximately 4 cm to T10 and rapidly inflated using an inflation device (Boston Scientific) to 8 atm of pressure. The balloon remained inflated for a 5-min period before being deflated and removed. The muscular wound was then sutured closed followed by closure of the skin with 9 mm surgical clips. An additional group of animals underwent all surgical procedures except inflation of the balloon catheter (sham, surgery controls).

BSCB permeability

Animals were assessed for BSCB permeability at 5 h ($n = 5$) or 24 h ($n = 4$) post-SCI (or sham, $n = 5$) using the Evan's Blue (EB) dye extravasation method as described previously.[14] Briefly, 30 min before perfusion, EB was injected intravenously. The animals were then perfused with saline under anesthesia and the spinal cord dissected; 10 mm segments were cut. Each segment was homogenized and the absorbance of the supernatant was measured at 610 nm using a spectrophotometer. The level of extravasated EB within each tissue sample was then determined using a previously obtained EB standard curve and was expressed as μg/g of spinal cord tissue.

Edema measurement

Animals were assessed for edema at 5 h ($n = 4$), 24 h ($n = 4$), or 3 days ($n = 4$) post-SCI (or sham, $n = 5$) using the wet weight/dry weight method as described previously.[14] Briefly, animals were administered a lethal injection of pentobarbital, and the spinal cord was removed rapidly. The spinal cord was cut into 10 mm segments, and the wet weight was obtained. Spinal cord segments were then oven dried at 100°C for 48 h before the dry weight was measured. The percentage of tissue water content was then calculated using the equation:

$$\%\ \text{Water Content} = \frac{(\text{Wet Weight} - \text{Dry Weight})}{\text{Wet Weight}} \times 100$$

ITP measurement

Animals (injured; $n = 6$, sham; $n = 5$) underwent a tracheotomy and the right and left femoral arteries were dissected. The right femoral artery was cannulated and connected to a syringe pump containing saline, which was administered at 2 mL/h except when taking a blood sample for blood gas analysis. A Codman MICROSENSOR intracranial pressure (ICP) probe was inserted into the left artery to monitor blood pressure. Immediately after balloon compression, another Codman MICROSENSOR ICP probe was introduced into the intrathecal space and extended to the injury epicenter. The laminectomy was then sealed with bone wax. The Codman probes were connected to an 8 channel Powerlab system (AD Instruments) and the output was viewed live and recorded with Labchart (AD Instruments). ITP was monitored for a 5-h period. Blood pressure and blood gases were monitored to ensure physiological parameters were maintained.

Functional outcome

Animals ($n = 12$) were assessed on days 3, 7, 10, and 14 post-SCI for both sensory and motor outcome.

The sensory prick test involved applying the tip end of Dumont #4 fine forceps to the shaved plantar surface of the hind paws. Animals were placed into an enclosed plastic box with a wire bottom where food was provided as a distraction. The fine forceps were applied to each hind paw 10 times with a 30-sec interval between each application. The response of the animal's withdrawal to the stimulus was graded as either; 0 = no response, 1 = weak response (slight movement of one joint of the hindlimb), 2 = moderate response (extensive movement of two or more joints of the hindlimb), or 3 = normal response. A sensory score out of 30 was given to each hind paw.

A modified Tarlov score[21] was used to assess motor function of the hindlimbs during a recorded 5-min monitoring period. The criteria were as follows: 0 = no movement; 1 = minor movement of the hindlimb joints; 2 = major movement of the hindlimb joints; 3 = able to stand properly but unable to hop; 4 = able to hop, but not properly; 5 = normal movement. To assess the frequency of any observed hindlimb movement, a forelimb to hindlimb ratio was calculated. The number of hindlimb movements per the first 20 forward moving forelimb steps was recorded. This ratio was then converted into a percentage.

Histological outcome

Animals ($n = 34$) were assessed for histological outcome using immunohistochemical techniques. Briefly, animals were perfuse fixed with 10% formalin at 5 h, 24 h, 3 days, or 2 weeks post-SCI. Spinal cord tissue was then processed and cut for assessment of morphological features (hematoxylin and eosin [H&E] stain), SP (Santa Cruz Sc-9758; 1:2000), NK1 receptor (Advanced Targeting Systems #AB-N33AP; 1:4000), albumin (Cappel #0113-0341; 1:20,000), microglia (Griffonia simplicifolia – Sigma L2140; 1:200), and aquaporin 4 (AQP4) (Abcam Ab9512; 1:200). All sections were scanned at high resolution using a Hamamatsu Nanozoomer. Slides were then viewed using the associated proprietary viewing software (NDP.view v1.1.27, Hamamatsu). Qualitative assessments were made by a blinded assessor using a ranking system (0 = no staining to 10 = extensive dark staining). Alternatively, whole cross-sections were exported and assessed using a color deconvolution method as described previously in detail elsewhere.[26]

Statistical analysis

EB extravasation, edema, ITP, plantar prick test, and color deconvolution were analyzed using a two-way analysis of variance (ANOVA) followed by Bonferroni post-tests. Such data was expressed as mean ± standard error of the mean (SEM). Immunohistochemistry ranking and modified Tarlov score were analysed using the Kruskal Wallis ANOVA followed by the Dunn multiple comparisons test. These data were expressed as the median and interquartile ranges.

Results

BSCB permeability – EB extravasation

Sham sections of spinal cord demonstrated minimal EB extravasation with only 6.93 ± 1.25 μg EB/g tissue measured (Fig. 1A). At 5 h post-SCI, a significant increase in EB extravasation was observed within the injury epicenter (15.43 ± 3.04 μg EB/g tissue) when compared with sham animals ($p < 0.001$). At 24 h post-SCI, a further increase in EB extravasation was observed within the injury epicenter (25.75 ± 10.11 μg EB/g tissue). This increase in permeability was significantly greater than that observed at 5 h ($p < 0.001$). At no time point post-SCI did the adjacent segments demonstrate EB extravasation.

Edema measurement

Sham sections recorded $65.55 \pm 2.08\%$ spinal cord water tissue content (Fig. 1B). At 5 h post-SCI, the percentage of spinal cord tissue water content within the injury epicenter significantly increased to $69.55 \pm 1.74\%$ when compared with sham animals ($p < 0.01$). Further increases were recorded at both 24 h ($71.73 \pm 1.31\%$, $p < 0.001$) and 3 days ($77.47 \pm 1\%$, $p < 0.001$) post-SCI, with water content at 3 days being significantly greater than 5 and 24 h post-injury. Further, by 3 days post-SCI, a significant increase in water content was observed within the adjacent segments when compared with sham animals (10 mm rostral = $p < 0.05$; 10 mm caudal = $p < 0.001$).

Intrathecal pressure

Sham animals demonstrated a low ITP recording of 0.65 ± 1.61 mm Hg when the probe was initially inserted immediately after deflation and removal of the balloon catheter and the laminectomy had been sealed with bone wax. Over the 5-h monitoring period, the ITP slightly increased and stabilized, reaching 3.75 ± 1.26 mm Hg by the end of monitoring (Fig. 1C). After SCI, an immediate significant increase ($p < 0.001$) in ITP was observed, reaching 5.31 ± 3.98 mm Hg. ITP continued to gradually rise over the 5-h monitoring period, reaching a maximal ITP of 7.36 ± 0.79 mm Hg by the end of monitoring. After injury, ITP was significantly increased at all time points when compared with sham ($p < 0.01$–0.001).

Functional outcome

Assessment of motor function confirmed that the surgical procedure did not affect motor function, with all sham animals obtaining a modified Tarlov score of 5 on all days post-SCI (Fig. 2A). Injured animals demonstrated a significant decrease in hindlimb motor function on all days post-SCI when compared with sham animals ($p < 0.01$). On days 3 and 6 post-SCI, each animal scored 0 with severe hindlimb paralysis observed. On days 10 and 14 post-SCI, all animals scored 1 with slight movement now observed in the hindlimbs; however, no further recovery of motor function was observed. Increases in the frequency of hindlimb movement (Fig. 2B) were apparent by day 6 post-SCI ($12.5\% \pm 9.87\%$) when compared with forelimb movement. On Day 14, this frequency increased further, reaching $20\% \pm 15.17\%$. On all days post-SCI, however, the frequency of hindlimb movement remained significantly worse compared with shams ($p < 0.001$).

Sham animals demonstrated normal sensory function after surgery (Fig. 2C), recording a score of 30 for each hindlimb on days 10 and 14 post-surgery. This result indicates that the surgical

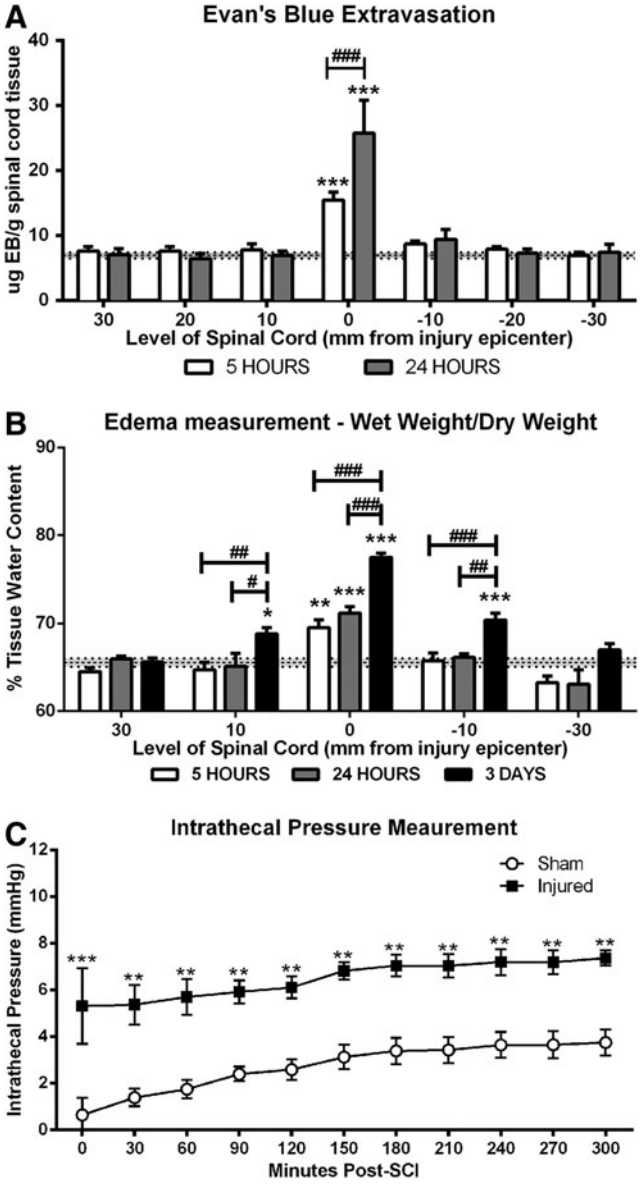

FIG. 1. (**A**) Evan's Blue (EB) extravasation was measured as an indicator of blood-spinal cord-barrier permeability. (**B**) The percentage of spinal cord tissue water content was measured to determine the extent of edema development post-SCI. (**C**) Intrathecal pressure recorded at the injury epicenter in both sham and injured animals for a 5-h monitoring period. Sham levels indicated by the dashed line in (A) and (B). *denotes $p < 0.05$, **denotes $p < 0.01$, ***denotes $p < 0.001$ when compared with sham. # denotes $p < 0.05$, ## denotes $p < 0.01$, ### denotes $p < 0.001$. SCI, spinal cord injury.

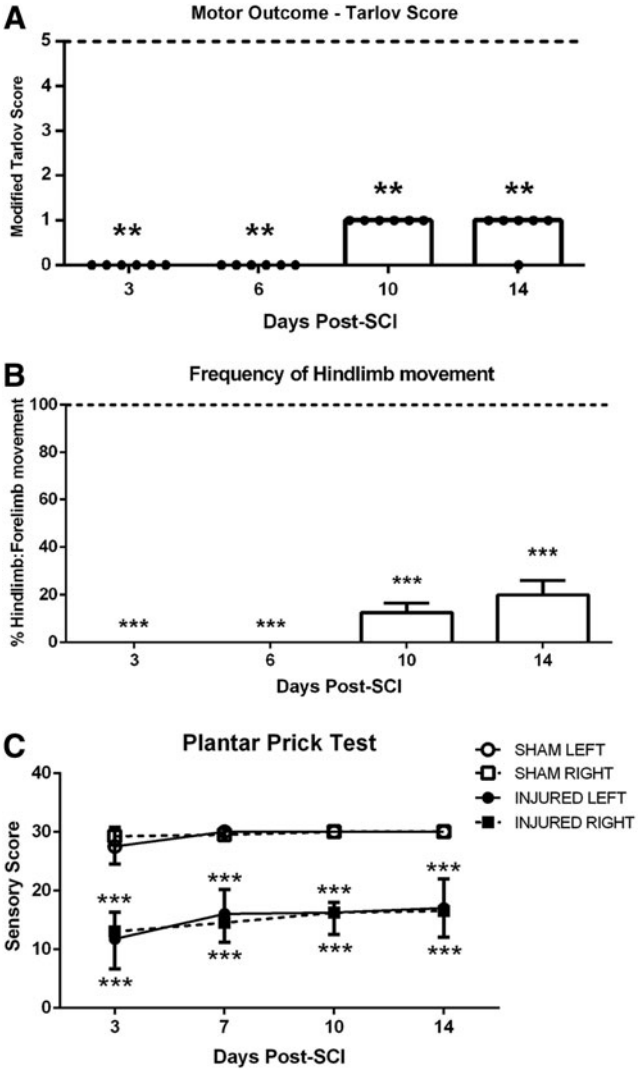

FIG. 2. Motor and sensory outcome after balloon compression spinal cord injury (SCI). (**A**) Motor function was assessed using the modified Tarlov score. (**B**) The frequency of observed hindlimb movement was also assessed, and while an increase in frequency was seen by day 14, this remained significantly reduced when compared with sham animals. (**C**) Sensory function deficits were assessed using the plantar prick test after injury in both the left and right hindlimbs. **denotes $p < 0.01$, ***denotes $p < 0.001$ when compared with sham.

procedure did not affect sensory function. The injured group demonstrated a significant decrease in sensory motor function at 3 days post-SCI, with a pain withdrawal score of 11.75 ± 4.57 and 13 ± 6.38 for the left and right hindlimbs, respectively ($p < 0.001$). Some spontaneous improvement was observed over the assessment period, and by day 14, the pain withdrawal score was 17 ± 4.96 and 16.5 ± 4.43 for the left and right hindlimbs, respectively ($p < 0.001$). No significant difference was observed between the left and right hindlimbs, indicating that a correctly placed central injury had occurred.

Morphological features – H&E staining

H&E staining was used to assess the general morphological features after balloon compression induced SCI (Fig. 3). At 5 h post-SCI, severe hemorrhage was present within the injury epicenter only, predominantly within the gray matter, with substantial tissue disruption apparent. By 24 h post-SCI, severe diffuse hemorrhage was still apparent within the injury epicenter, and greater loss of tissue architecture was observed. Hemorrhage had also spread to the adjacent segments by this time. By 3 days post-SCI, diffuse hemorrhage was reduced within the injury epicenter, while localied hemorrhage was still seen within the adjacent segments. At 2 weeks post-SCI, extensive tissue loss was evident with cavity formation and minimal white matter sparing. The adjacent segments also demonstrated loss of tissue, centered within the gray matter and radiating outward.

SP immunoreactivity

Two specific regions of SP immunoreactivity were assessed—namely, the dorsal horn region where SP is known to be stored, and the perivascular region to determine if SP was associated with BSCB permeability after SCI (Fig. 4). Sham animals demonstrated a moderate level of SP immunoreactivity (median ranking = 6) within the gray matter with predominance in lamina I and II of the dorsal horn. At 5 h post-SCI, a significant decrease (median ranking = 2) was observed within the injury epicenter when compared with sham. The adjacent segments also demonstrated reduced SP immunoreactivity, with both 10 mm caudal and rostral significantly decreasing to a median of 4. Similarly, at 30 mm caudal and rostral to the injury epicenter, a slight decrease was observed (median ranking = 5 and 4, respectively). SP immunoreactivity was maximally decreased within the injury epicenter by 24 h post-SCI, with a median ranking of 0 ($p < 0.001$). Thereafter, SP immunoreacitivity remained absent at both 3 days and 2 weeks post-SCI. SP loss extended along the cord and was observed out to 30 mm caudal and rostral.

Perivascular SP immunoreactivity was assessed within the gray matter of the spinal cord, although the injury epicenter could not be examined because of severe tissue disruption. Sham animals demonstrated moderate SP intensity with a median ranking of 6. At 5 h post-SCI, only a slight decrease was observed within the adjacent segments. At 24 h post-SCI, a further reduction in both the caudal and rostral directions was observed, with rostral segments recording a slightly greater decrease (median = 4) compared with caudal segments (median = 5). By 3 days post-SCI, all adjacent segments had reduced SP immunoreactivity recording a median ranking of 4. By 2 weeks post-SCI, rostral segments had returned to sham levels, while the caudal segments still remained slightly below sham levels.

NK1 immunoreactivity

Two regions were assessed for NK1 receptor immunoreactivity—namely, the gray matter and the perivascular region within the white matter (Fig. 5). Sham sections demonstrated moderate diffuse staining within the gray matter with intense staining observed within the dorsal horn. At 5 and 24 h post-SCI, a significant increase within the injury epicenter to a median ranking of 9 was observed throughout the entire cross-sections ($p < 0.001$). At this time, a slight increase in the proximal adjacent segments was observed while the more distal adjacent segments showed reduced immunoreactivity. By 3 days post-SCI, diffuse immunoreactivity was apparent, although no longer significantly different to shams. All adjacent segments demonstrated reduced immunoreactivity when compared with shams, with 30 mm rostral obtaining a median ranking of 5. By 2 weeks post-SCI, a significant loss of tissue within

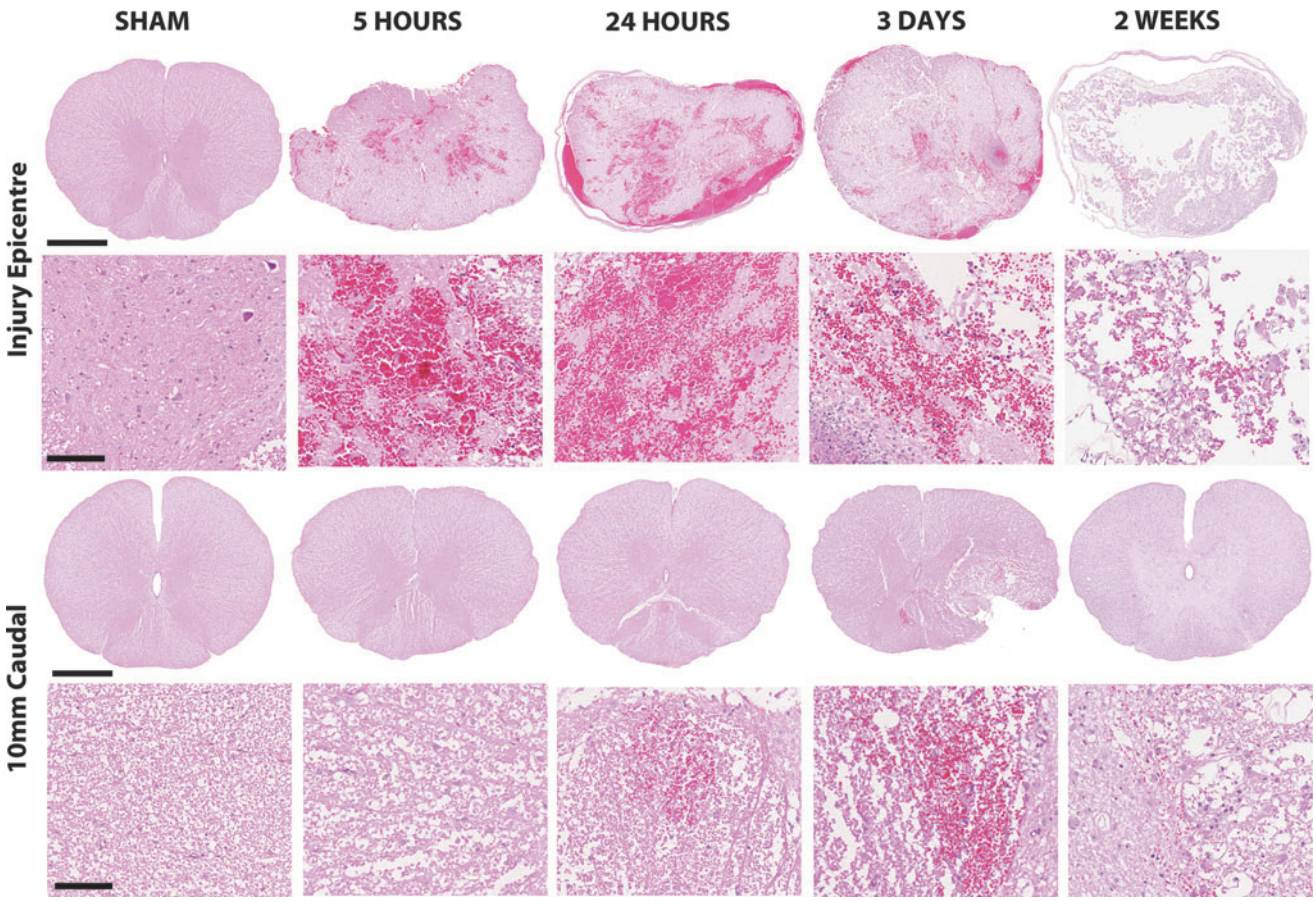

FIG. 3. Hematoxylin and eosin staining demonstrates the morphological changes in both the injury epicenter and adjacent injury from 5 h to 2 weeks post-SCI. Cross-section scale bar = 1 mm; high magnification scale bar = 100 μm. Color image is available online at www.liebertpub.com/neu

the injury epicenter meant no analysis of the gray matter region could be undertaken. The adjacent segments, however, demonstrated a significant decrease in NK1 immunoreactivity with both proximal adjacent segments obtaining a median ranking of 4 (rostral = $p < 0.01$, caudal $p < 0.001$).

Within the perivascular region, sham sections demonstrated faint NK1 receptor immunoreactivity with a median ranking of 4. At 5 h post-SCI, there was only a slight increase in NK1 immunoreactivity seen within any section. By 24 h post-SCI, a marked increase in NK1 receptor immunoreactivity was observed in all adjacent segments apart from 30 mm caudal, which demonstrated decreased immunoreactivity to a median ranking of 3. By day 3 post-SCI, however, NK1 immunoreactivity in this section had returned to above sham levels. The 10 mm caudal was also increased, whereas both rostral segments had returned to sham levels. By 2 weeks post-SCI, all adjacent segments were comparable to sham levels except for 30 mm caudal, which remained increased with a median ranking of 6. Note that the injury epicenter of injured animals was not assessable because of tissue disruption.

Albumin immunoreactivity

Sham sections demonstrated minimal albumin immunoreactivity with a DABwt% by color deconvolution of 4.7 ± 0.42 (Fig. 6). At 5 h post-SCI, a significant increase was observed within the injury epicenter (22.09 ± 1.25 DABwt%; $p < 0.001$) and proximal adjacent segments (10 mm rostral = 7.72 ± 1.53 DABwt%, $p < 0.05$; 10 mm caudal = 9.58 ± 3.93 DABwt%, $p < 0.001$). At 24 h post-SCI, albumin immunoreactivity was maximal within the injury epicenter (24.64 ± 2.77 DABwt%; $p < 0.001$) and proximal adjacent segments (DABwt% = 10.68 ± 1.99 and 11.33 ± 3.08, respectively; $p < 0.001$). At 3 days post-SCI, albumin immunoreactivity decreased within the injury epicenter, although remained significantly greater than sham levels (DABwt% = 13.09 ± 1.79; $p < 0.001$). At this time, 10 mm caudal remained significantly above sham levels (DABwt% = 8.73 ± 3.13; $p < 0.001$); however, 10 mm rostral became comparable to sham (DABwt% = 6.76 ± 1.03). At 2 weeks post-SCI, all adjacent segments of spinal cord remained comparable to sham, while the injury epicenter remained significantly elevated (DABwt% = 9.05 ± 2.43; $p < 0.001$).

Microglial immunoreactivity (ISOB4)

Within the spinal cord white matter, sham sections demonstrated small numbers of resting microglia with long fine processes (Fig. 7). At 24 h post-SCI, many small round cells were seen and are indicative of phagocytic microglia. Further, increased immunoreactivity was also apparent within the adjacent segments at this time. By 3 days and 2 weeks post-SCI, marked tissue loss was observed within the injury epicenter, and florid microglia awee present within the white matter, becoming amoeboid in shape by 2 weeks. The adjacent segments of spinal cord also demonstrated a gradual increase in microglia over time, with the greatest immunoreactivity observed at 2 weeks post-SCI.

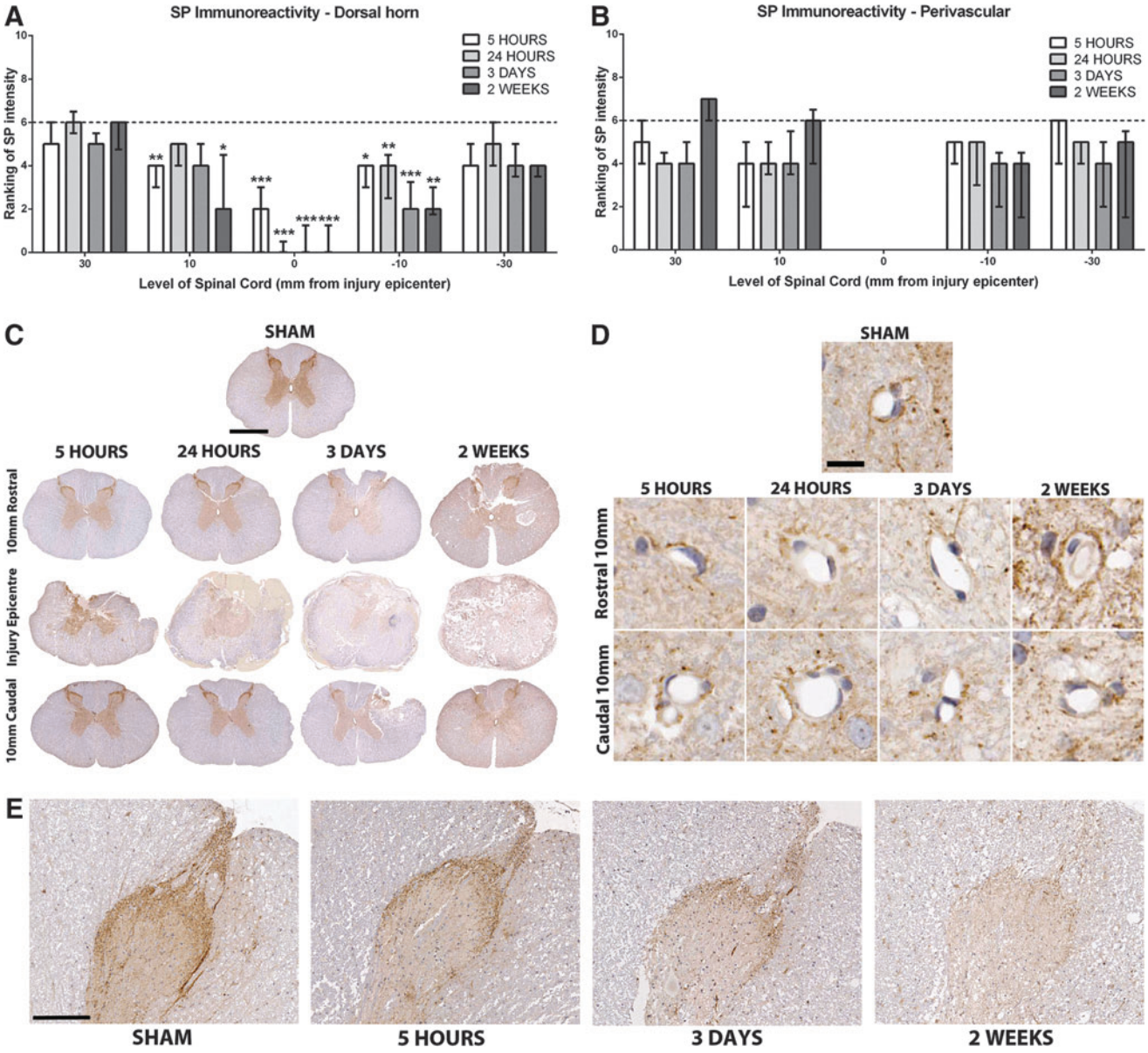

FIG. 4. Assessment of substance P (SP) immunoreactivity within the dorsal horn and perivascular region after balloon compression spinal cord injury. (**A**) Ranking of SP immunoreactivity within the dorsal horn region of the spinal cord demonstrated a marked decrease within the injury epicenter at all time points post-injury (A, **C**). Ranking of SP immunoreactivity within the perivascular region (**B, D**) demonstrated a moderate decrease after injury. (**E**) Higher magnification images of SP within the dorsal horn region (scale bar = 200 μm). # denotes $p < 0.05$, ## denotes $p < 0.01$, ### denotes $p < 0.001$ when compared with sham (indicated by the dashed line). Scale bar = 1 mm (C), 25 μm (D). Color image is available online at www.liebertpub.com/neu

Within the gray matter, sham sections of spinal cord demonstrated a small amount of resting microglial immunoreactivity with long fine processes. At 5 and 24 h post-SCI, increased small round cells could be seen within the injury epicenter, which are likely infiltrating phagocytic microglia. The adjacent segments demonstrated an increase in microglial immunoreactivity, particularly surrounding blood vessels. By 3 days post-SCI, greater tissue loss was observed within the injury epicenter, with many round phagocytic microglia present. The adjacent segments demonstrated increasing numbers of activated microglia that appeared ramified in nature. By 2 weeks post-SCI, increased tissue loss was observed within the injury epicenter, with larger phagocytic cells noted. The adjacent segments demonstrated increased microglial activity, with many fully ramified and amoeboid in appearance.

AQP4 immunoreactivity

Two specific regions were assessed for AQP4 immunoreactivity—namely, the perivascular region and the central canal region (Fig. 8). At 5 h post-SCI, increased AQP4 immunoreactivity was observed in all adjacent segments of the spinal cord. The injury epicenter was too disrupted to analyze the vasculature of the gray matter. By 24 h post-SCI, a further increase in AQP4 immunoreactivity was seen within the caudal adjacent segments, reaching a median ranking of 6. The rostral segments remained elevated above

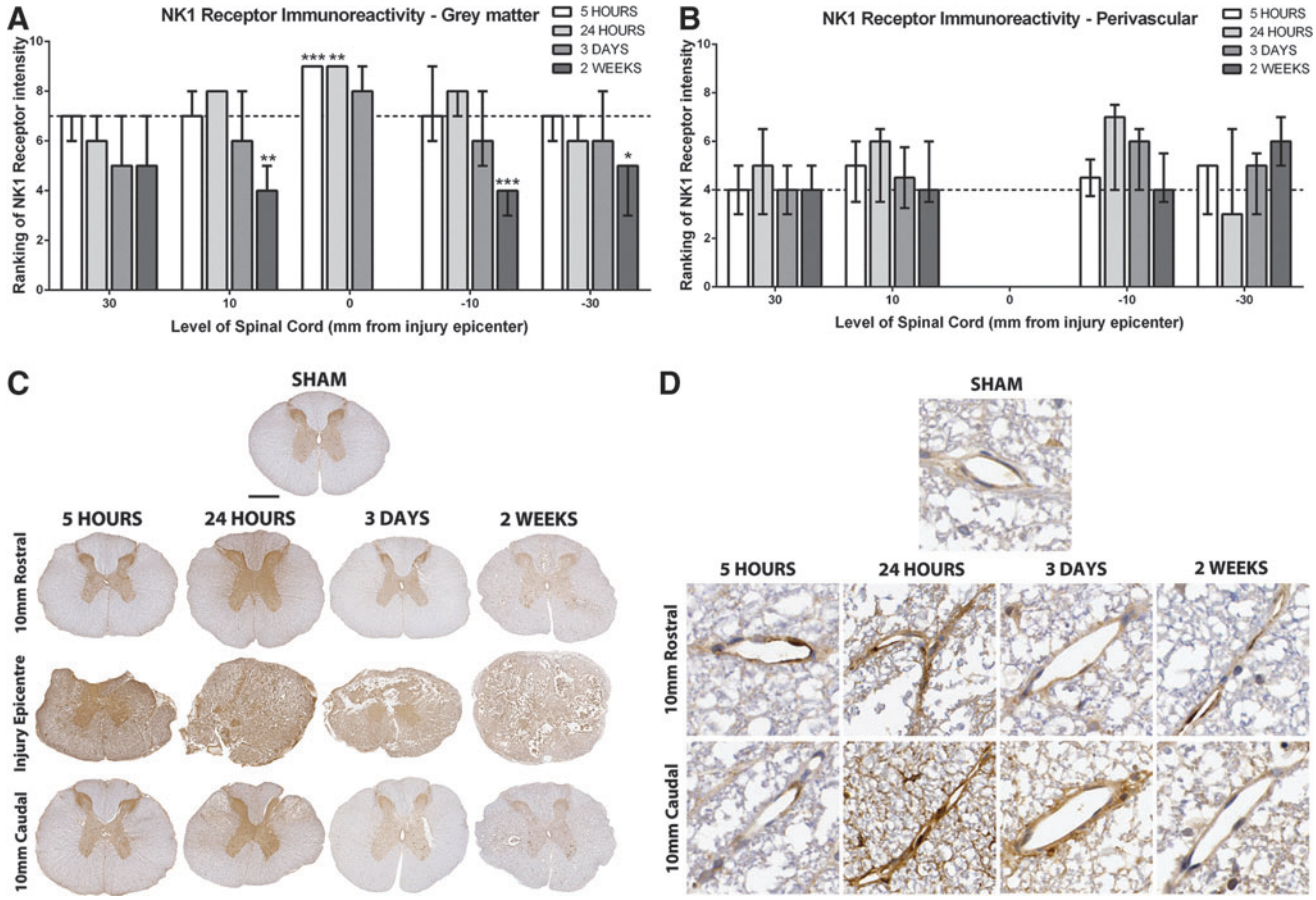

FIG. 5. Assessment of NK1 receptor immunoreactivity after balloon compression spinal cord injury (SCI). NK1 receptor immunoreactivity initially increased within the gray matter of the injury epicenter and proximal adjacent segments (**A, C**); however by 3 days post-SCI, a reduction was observed that became significant by 2 weeks. Perivascular NK1 receptor immunoreactivity (**B, D**) demonstrated an initial increase within the proximal adjacent segments before returning to sham levels. # denotes $p < 0.05$, ## denotes $p < 0.01$, ### denotes $p < 0.001$ when compared with sham (indicated by the dashed line). Scale bar = 1 mm (C), 50 μm (D). Color image is available online at www.liebertpub.com/neu

sham levels, with a median of 5. By 3 days post-SCI, the caudal segments approached sham levels, with a median ranking of 4. By 2 weeks post-SCI, a significant decrease to a median of 1 was observed at 10 mm caudal. In addition, 30 mm caudal and 10 mm rostral also demonstrated reduced AQP4 immunoreactivity while 30 mm rostral remained comparable to sham levels.

The central canal region demonstrated faint AQP4 immunoreactivity within the ependymal cells of sham sections with a median ranking of 3. At 5 h post-SCI, a slight increase was observed at 10 mm rostral to a median of 4.5, while 30 mm rostral and caudal demonstrated a small increase to a median of 4. At 24 h post-SCI, further increases were observed with 30 mm rostral ($p < 0.01$) and 10 mm caudal obtaining a median ranking of 6, while 10 mm rostral and 30 mm caudal had a median ranking of 5. By 3 days post-SCI, all adjacent segments remained elevated above sham, with a median ranking of 5. By 2 weeks post-SCI, AQP4 immunoreactivity had decreased to near sham levels.

Discussion

The balloon compression model of SCI was first described by Tarlov and Klinger[21] in dogs, and later adapted to cats,[27] rats,[24] and primates.[28] Such studies have demonstrated that the severity of the balloon compression directly correlates to lesion size and behavioral deficits. This model has since been described in rabbits,[29] although characterization has not been extensive. In the current study, balloon compression SCI produced significant motor deficits with minimal recovery observed over the 2-week assessment period. While this represents the severe end of the neurological deficit scale, it is an ideal injury severity for assessment of therapeutic interventions, because any observed improvements can be attributed to the intervention as opposed to spontaneous recovery. Frequency of hindlimb movement was additionally measured to more accurately assess the extent of functional recovery. Frequency of hindlimb movement increased from day 10 to day 14 post-SCI, despite no improvement in the Tarlov score. As such, frequency of hindlimb movement represents an important additional outcome measure of functional recovery that should be examined in conjunction with the modified Tarlov score to provide a more accurate assessment.

During assessment of sensory function, it was noted that the Von Frey hair test and Hargreaves heat test, commonly used in both rat and mouse models of SCI,[30] did not elicit a response in sham animals. As such, the plantar prick test was used. This test showed a significant loss in sensory function after SCI with minimal improvement over the 2-week assessment period. No significant difference was seen between the left and right hindlimbs, indicating a consistent central placement of the balloon catheter, which was easily reproducible. The significant reduction in motor function

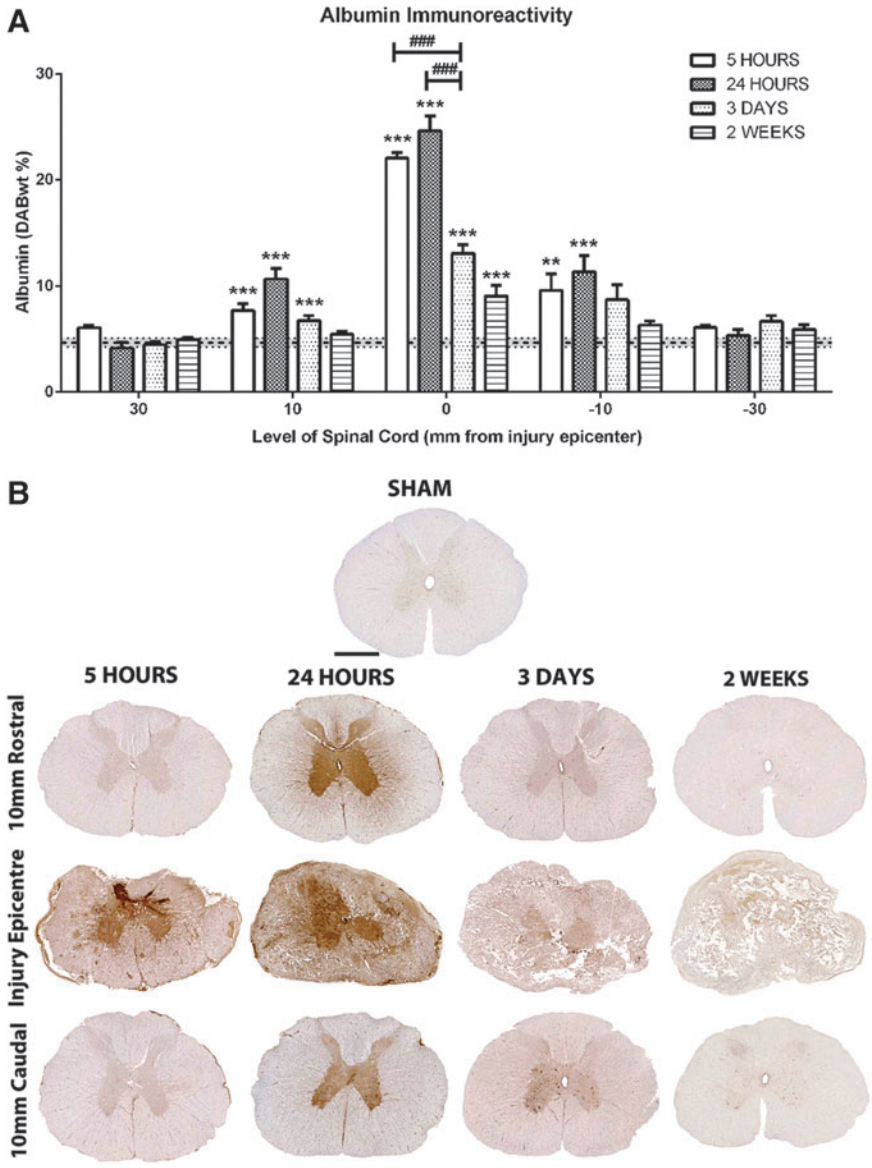

FIG. 6. Albumin immunoreactivity after balloon compression SCI. Assessment of albumin immunoreactivity using color deconvolution (**A**) demonstrated a significant increase at all time points post-injury within the injury epicenter (**B**). Further, significant increases were observed 10 mm rostral and caudal at both 5 and 24 h post-SCI. ** denotes $p < 0.01$, *** denotes $p < 0.001$ compared with sham (indicated by the dashed line). ### denotes $p < 0.001$ between indicated groups. Scale bar = 1 mm. Color image is available online at www.liebertpub.com/neu

observed may have impaired the ability of animals to withdraw the hindlimb. Sudden changes in behavior, such as ceasing eating or looking toward the hindlimb, however, were not observed when no response was elicited. Overall, the balloon compression model produced consistent motor and sensory deficits with minimal spontaneous recovery by 2 weeks post-injury.

The observed loss in neurological function after the balloon compression model of SCI can be attributed to the pathological features apparent after histological examination. Severe hemorrhage was observed early post-SCI, extending into the adjacent segments, with cystic cavitation apparent by 2 weeks post-SCI. Such pathological features have previously been described in many studies using the balloon compression model[24] and other experimental models of SCI such as the weight drop[31] and clip compression.[32] Further, the observed pathological features are similar to those described after human SCI.[33]

Microglia have also been implicated in contributing to further cell death after SCI. Indeed, numerous *in vitro* studies have demonstrated that microglia release factors that promote cell death such as glutamate,[34] tumor necrosis factorα,[34] nitric oxide,[35] interleukin-1β,[36] and reactive oxygen species.[37] Our results demonstrate early increases in microglial numbers predominantly in the penumbra of the injury epicenter. Previous studies have similarly demonstrated that microglia populations proliferate aafter SCI.[38] The early increased microglial population and phagocytic appearance by 2 weeks post-SCI correlates to the loss of neuronal cells by this time, thus implicating a role for microglia in contributing to secondary cell death after balloon compression SCI.

Importantly, this study assessed the development of neurogenic inflammation after traumatic SCI. It has now been well documented that SP mediates the development of neurogenic inflammation after both TBI and stroke.[13,15–17,20] Indeed, blockade of SP through

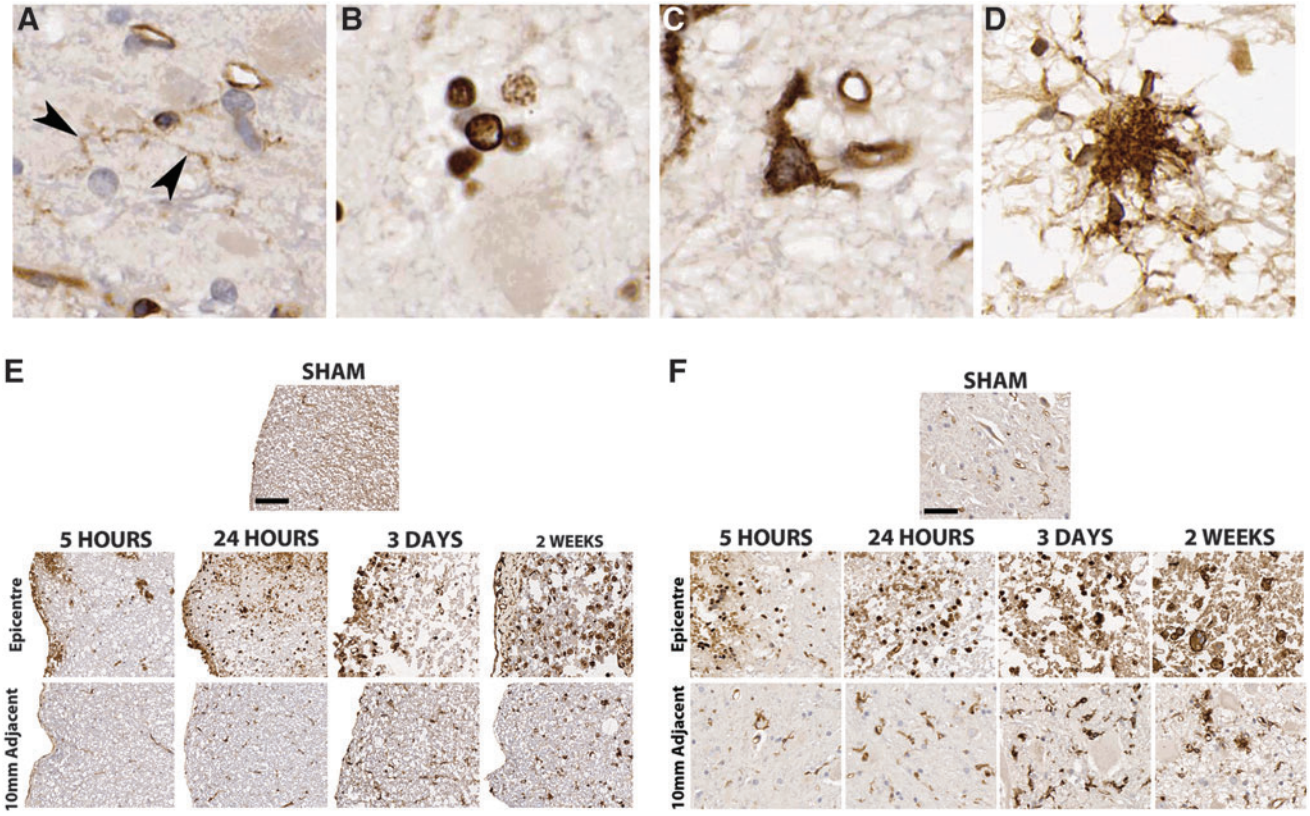

FIG. 7. Microglial immunoreactivity after balloon compression spinal cord injury (SCI). Representative images of microglial types observed were: (**A**) resting microglia with fine long processes (arrows); (**B**) small round phagocytic cells present within areas of severe hemorrhage; (**C**) activated microglia with short ramified processes; (**D**) fully activated microglia with very short ramified processes and amoeboid shape suggestive of phagocytic activity. Within the white matter (**E**), increased microglia are present within the injury epicenter and adjacent segments post-injury. Within the gray matter (**F**), increased small round microglia can be seen within the injury epicenter after injury. The adjacent segments demonstrate ramified microglia by 3 days post-SCI, which appear fully ramified by 2 weeks post-SCI. Scale bar = 200 μm (E), 50 μm (F). Color image is available online at www.liebertpub.com/neu

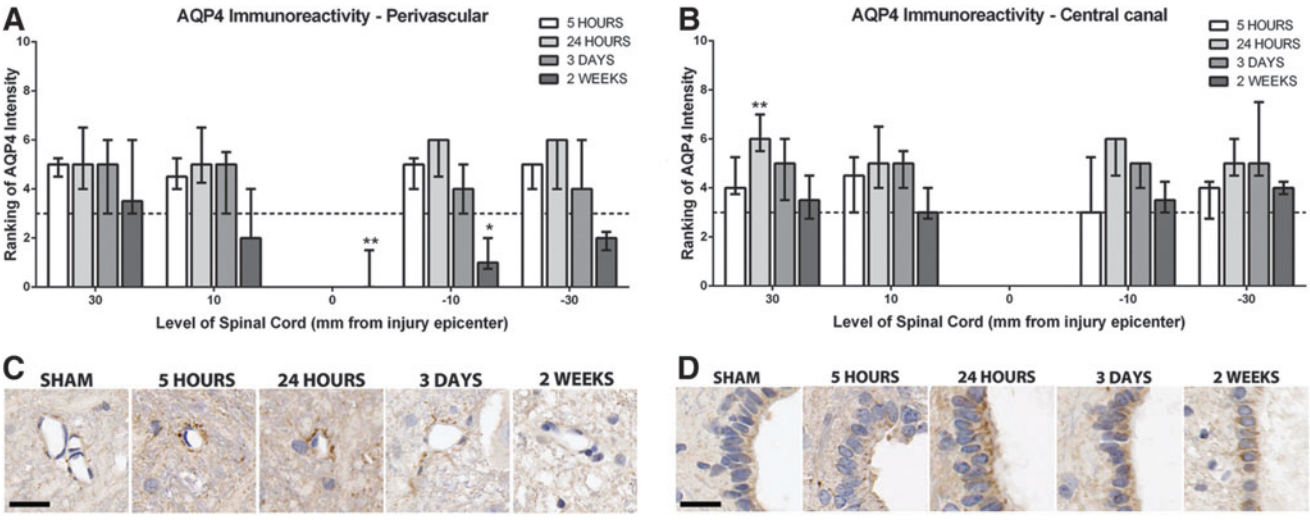

FIG. 8. AQP4 immunoreactivity after balloon compression SCI. AQP4 immunoreactivity within the perivascular (**A, C**) and central canal region (**B, D**) of the spinal cord post-injury. Note that images are within the immediately adjacent segments, because the injury epicenter was severely disrupted. Scale bar = 25 μm (C, D). Color image is available online at www.liebertpub.com/neu

inhibition of the NK1 receptor resulted in reduced barrier permeability and edema, and improved functional outcome. Reduced SP immunoreactivity observed within the current study may be largely from severe tissue disruption. Nonetheless, intact spinal cord adjacent to the injury site exhibited declines in SP immunoreactivity, maximal at 3 days post-injury. Similar results have been reported after a weight drop model, with maximal SP decreases found at 1 week post-injury.[39] In addition, after a transection model of SCI, SP decreased within the injury epicenter, although increased caudal to the lesion site.[40] In contrast, our own results show that perivascular SP was comparable to sham levels rostral to the lesion site by 2 weeks post-SCI while caudal segments demonstrated reduced SP. Taken together, these results demonstrate the varying response of SP to injury induced by different models. Indeed, a model of transient spinal cord ischemia in the rabbit resulted in no change in SP expression,[41] emphasizing the requirement of mechanical trauma to induced alterations in SP expression after injury.

Our own results suggest that SP is released from the dorsal horn stores after injury as indicated by the gradual depletion of SP over time. Interestingly, the perivascular immunoreactivity demonstrated a decline in SP fter injury, which differs from previous investigations after TBI and stroke where an increase was observed.[13,16,17] Sharma and colleagues[40] demonstrated increased SP at 1–2 h post-SCI within the dorsal horn, suggesting an earlier time point may be needed to observe such an increase. In addition, the binding of SP to the NK1 receptor causes internalization[42] and thus may contribute to the observed reduction in perivascular immunoreactivity.

The localization of the NK1 receptor in the spinal cord has been extensively studied, with the highest expression found within the dorsal horn, intermediolateral cell column, and lamina X.[43] The current study is the first to assess the response of the NK1 receptor after balloon compression. Consistent with previous studies, our results demonstrate high NK1 immunoreactivity within the dorsal horn region of the gray matter. After injury, the initial increase in NK1 immunoreactivity may have been in response to the release of SP, resulting in an up-regulation of its receptor. Indeed, after a transection model of SCI, an up-regulation of both the NK1 receptor[44] and SP[40] have been reported below the lesion level. After binding and activation of the receptor, internalization of both the receptor and ligand occurs,[42] thus potentially causing the later reduction in NK1 receptor immunoreactivity. Taken together, both the changes in SP and NK1 receptor immunoreactivity support the development of SP mediated neurogenic inflammation after SCI.

The process of neurogenic inflammation is characterized by vasodilation, plasma protein extravasation, and edema.[45] Recent studies after both TBI and stroke have demonstrated increased SP immunoreactivity that is associated with BBB disruption, vasogenic edema, and worsened neurological function.[13,16,17] The current study demonstrated significantly increased BSCB permeability at 5 and 24 h post-injury as determined by EB extravasation and albumin immunoreactivity. Such results are consistent with previous studies after weight drop,[46] clip compression,[47] transection,[48] and forceps compression[49] models of SCI. Increased barrier permeability early post-injury is likely from mechanical disruption given the severe hemorrhage observed. Increased BSCB was observed, however, within the intact adjacent segments, indicating a spread of barrier disruption in a rostrocaudal direction. Such results are consistent with previous experiments where BSCB permeability was apparent within spinal segments beyond the injury site.[10]

Our own study demonstrated that albumin immunoreactivity was confined to the injury epicenter by 2 weeks post-injury, implicating restoration of the barrier within the adjacent segments. While these results support previous investigations in which BSCB permeability was gradually restored over time,[50] considerable debate remains over the timing of BSCB restoration. Some studies have proposed that a second phase of BSCB permeability transpires after injury as early as 3 days post-SCI.[51] In comparison, Popovich and colleagues[52] have demonstrated that a second phase of BSCB permeability occurs later at 28 days after injury, presumably because of revascularization. Given the acute assessment period in the current study, however, no further alterations in BSCB permeability were observed.

Increased BSCB permeability leads to the development of vasogenic edema, which has been well characterized after severe SCI, initially within the epicenter[53] followed by delayed spread to the adjacent segments.[7,8] Within the current study, increased edema was limited to the injury epicenter at 5 and 24 h post-SCI. At 3 days post-SCI, however, a greater increase was observed within the epicenter, with rostrocaudal spread into the uninjured adjacent segments. Such changes have previously been described[7] and are thought to be from ultrafiltration rather than exudation that occurs in vasogenic edema. Our own results support this theory, because the rostrocaudal spread of edema was associated with minimal extravasation of albumin, suggesting that such edema was not vasogenic in nature.

An alternate concept of edema development after SCI implicates the involvement of the water channel protein, AQP4. In a cold lesion brain injury[54] and contusion SCI[55] model, AQP4-null mice demonstrated increased edema development and worsened neurological outcome. Such results allude to a protective role of AQP4 in facilitating the removal of excess water. In contrast, after a forceps compression model, AQP4 null mice demonstrated reduced edema and improved neurological function,[12] thus implicating a role for AQP4 in facilitating water entry into the spinal cord tissue. Up-regulation of AQP4, however, has been associated with reduced edema development in both contusion[2] and clip compression models,[56] thus supporting a role for AQP4 in water clearance after SCI. The current study demonstrated an initial increase in AQP4 immunoreactivity as far as 30 mm from the injury epicenter and suggests it may be responsible for the increased edema development within the adjacent segments. Alternatively, increased AQP4 may be compensatory to facilitate water clearance. Modulation of AQP4 through application of either antagonists or agonists is needed to better elucidate the role of AQP4 in edema development after SCI.

The development of edema after SCI may result in a detrimental increase in ITP, subsequently reducing blood perfusion and contributing to further tissue damage.[1] The extent of ITP attributed damage is debated, given that the vertebral canal provides some space to accommodate edematous expansion.[57] The current study, however, certainly demonstrates increased ITP after balloon compression SCI. The immediate ITP increase was likely caused by an expansion of volume because of the severe hemorrhage observed. Increased ITP was also apparent over time, however, which given the increase in edema at 5 h, may be because of such edema development. Previous studies have similarly demonstrated increases in ITP after SCI that were associated with reduced blood flow and increased tissue damage.[12] Further, immediate cerebrospinalfluid drainage to reduce raised ITP resulted in significantly smaller areas of tissue damage 4 weeks after a contusion injury.[58] Similarly, Saadoun and colleagues[12] demonstrated that AQP4 deficient mice exhibited reduced edema and spinal cord pressure when compared with wildtype mice. As such, ITP

contributes to greater tissue damage and functional deficits post-SCI and subsequently may represent an important target for future therapeutic interventions.

Given the significant contribution of ITP to the continued development of injury after SCI, the use of an injury model that replicates the closed environment of a clinical injury is vital. Moreover, Batchelor and coworkers[59] demonstrated that local rises in intracanal pressure were a determinant for poor neurological outcome and greater tissue injury, confirming ITP as an important injury mechanism in which current research is limited. The current study has demonstrated that the balloon compression model produces increases in ITP that may otherwise be absent in open injury models. Further, the balloon compression model replicates important primary injury mechanisms such as an initial impact followed by continued compression, which are present in human SCI. These differences in injury processes and environment may contribute to the novel findings in this study.

Conclusion

The current study has demonstrated that the balloon compression model replicates many facets of human SCI while replicating the closed environment of human injury. As such, the balloon compression model of SCI represents an important injury model for future use within the SCI field. Further, these results implicate the AQP4 water channel protein in the development of edema after injury. The changes described in the present study were associated with alterations in the immunoreactivity of SP and the NK1 receptor, thus suggesting a role for SP as a mediator of neurogenic inflammation after SCI. SP may thus be a potential therapeutic target to inhibit neurogenic inflammation after injury.

Acknowledgment

Supported in part by the Neil Sacshe Foundation, Australia.

Author Disclosure Statement

No competing financial interests exist.

References

1. Sharma, H.S. (2005). Pathophysiology of blood-spinal cord barrier in traumatic injury and repair. Curr. Pharm. Des. 11, 1353–1389.
2. Nesic, O., Lee, J., Ye, Z., Unabia, G.C., Rafati, D., Hulsebosch, C.E., and Perez-Polo, J.R. (2006). Acute and chronic changes in aquaporin 4 expression after spinal cord injury. Neuroscience 143, 779–792.
3. Sharma, H.S., Winkler, T., Stalberg, E., Olsson, Y., and Dey, P.K. (1991). Evaluation of traumatic spinal cord edema using evoked potentials recorded from the spinal epidural space. An experimental study in the rat. J. Neurol. Sci. 102, 150–162.
4. Sharma, H.S., Olsson, Y., Nyberg, F., and Dey, P.K. (1993). Prostaglandins modulate alterations of microvascular permeability, blood flow, edema and serotonin levels following spinal cord injury: an experimental study in the rat. Neuroscience 57, 443–449.
5. Winkler, T., Sharma, H.S., Stalberg, E., Olsson, Y., and Nyberg, F. (1994). Opioid receptors influence spinal cord electrical activity and edema formation following spinal cord injury: experimental observations using naloxone in the rat. Neurosci. Res. 21, 91–101.
6. Ates, O., Cayli, S.R., Gurses, I., Turkoz, Y., Tarim, O., Cakir, C.O., and Kocak, A. (2007). Comparative neuroprotective effect of sodium channel blockers after experimental spinal cord injury. J. Clin. Neurosci. 14, 658–665.
7. Nemecek, S., Petr, R., Suba, P., Rozsival, V., and Melka, O. (1977). Longitudinal extension of oedema in experimental spinal cord injury—evidence for two types of post-traumatic oedema. Acta. Neurochir. (Wien) 37, 7–16.
8. Demediuk, P., Lemke, M., and Faden, A.I. (1990). Spinal cord edema and changes in tissue content of Na+, K+, and Mg2+ after impact trauma in rats. Adv. Neurol. 52, 225–232.
9. Wang, R., Ehara, K., and Tamaki, N. (1993). Spinal cord edema following freezing injury in the rat: relationship between tissue water content and spinal cord blood flow. Surg. Neurol. 39, 348–354.
10. Noble, L.J., and Wrathall, J.R. (1989). Distribution and time course of protein extravasation in the rat spinal cord after contusive injury. Brain Res. 482, 57–66.
11. Goodman, J.H., Bingham, W.G., Jr., and Hunt, W.E. (1976). Ultrastructural blood-brain barrier alterations and edema formation in acute spinal cord trauma. J. Neurosurg. 44, 418–424.
12. Saadoun, S., Bell, B.A., Verkman, A.S., and Papadopoulos, M.C. (2008). Greatly improved neurological outcome after spinal cord compression injury in AQP4-deficient mice. Brain 131, 1087–1098.
13. Donkin, J.J., Nimmo, A.J., Cernak, I., Blumbergs, P.C., and Vink, R. (2009). Substance P is associated with the development of brain edema and functional deficits after traumatic brain injury. J. Cereb. Blood Flow Metab. 29, 1388–1398.
14. Vink, R., Young, A., Bennett, C.J., Hu, X., Connor, C.O., Cernak, I., and Nimmo, A.J. (2003). Neuropeptide release influences brain edema formation after diffuse traumatic brain injury. Acta. Neurochir. Suppl 86, 257–260.
15. Nimmo, A.J., Cernak, I., Heath, D.L., Hu, X., Bennett, C.J., and Vink, R. (2004). Neurogenic inflammation is associated with development of edema and functional deficits following traumatic brain injury in rats. Neuropeptides 38, 40–47.
16. Turner, R.J., Blumbergs, P.C., Sims, N.R., Helps, S.C., Rodgers, K.M., and Vink, R. (2006). Increased substance P immunoreactivity and edema formation following reversible ischemic stroke. Acta. Neurochir. Suppl 96, 263–266.
17. Corrigan, F., Leonard, A., Ghabriel, M., Van Den Heuvel, C., and Vink, R. (2012). A substance P antagonist improves outcome in female Sprague Dawley rats following diffuse traumatic brain injury. CNS Neurosci. Ther. 18, 513–515.
18. Harford-Wright, E., Thornton, E., and Vink, R. (2010). Angiotensin-converting enzyme (ACE) inhibitors exacerbate histological damage and motor deficits after experimental traumatic brain injury. Neurosci. Lett. 481, 26–29.
19. Thornton, E., and Vink, R. (2012). Treatment with a substance P receptor antagonist is neuroprotective in the intrastriatal 6-hydroxydopamine model of early Parkinson's disease. PLoS One 7, e34138.
20. Turner, R.J., Helps, S.C., Thornton, E., and Vink, R. (2011). A substance P antagonist improves outcome when administered 4 h after onset of ischaemic stroke. Brain Res. 1393, 84–90.
21. Tarlov, I.M., and Klinger, H. (1954). Spinal cord compression studies. II. Time limits for recovery after acute compression in dogs. AMA Arch. Neurol. Psychiatry 71, 271–290.
22. Tarlov, I.M., Klinger, H., and Vitale, S. (1953). Spinal cord compression studies. I. Experimental techniques to produce acute and gradual compression. AMA Arch. Neurol. Psychiatry 70, 813–819.
23. Fukuda, S., Nakamura, T., Kishigami, Y., Endo, K., Azuma, T., Fujikawa, T., Tsutsumi, S., and Shimizu, Y. (2005). New canine spinal cord injury model free from laminectomy. Brain Res. Brain Res. Protoc. 14, 171–180.
24. Martin, D., Schoenen, J., Delree, P., Gilson, V., Rogister, B., Leprince, P., Stevenaert, A., and Moonen, G. (1992). Experimental acute traumatic injury of the adult rat spinal cord by a subdural inflatable balloon: methodology, behavioral analysis, and histopathology. J. Neurosci. Res. 32, 539–550.
25. Vanicky, I., Urdzikova, L., Saganova, K., Cizkova, D., and Galik, J. (2001). A simple and reproducible model of spinal cord injury induced by epidural balloon inflation in the rat. J. Neurotrauma 18, 1399–1407.
26. Helps, S.C., Thornton, E., Kleinig, T.J., Manavis, J., and Vink, R. (2012). Automatic nonsubjective estimation of antigen content visualized by immunohistochemistry using color deconvolution. Appl. Immunohistochem. Mol. Morphol. 20, 82–90.
27. Martin, S.H., and Bloedel, J.R. (1973). Evaluation of experimental spinal cord injury using cortical evoked potentials. J. Neurosurg. 39, 75–81.
28. Nesathurai, S., Graham, W.A., Mansfield, K., Magill, D., Sehgal, P., Westmoreland, S.V., Prusty, S., Rosene, D.L., and Sledge, J.B. (2006). Model of traumatic spinal cord injury in Macaca fascicularis: similarity of experimental lesions created by epidural catheter to human spinal cord injury. J. Med. Primatol. 35, 401–404.

29. Aslan, A., Cemek, M., Buyukokuroglu, M.E., Altunbas, K., Bas, O., Yurumez, Y., and Cosar, M. (2009). Dantrolene can reduce secondary damage after spinal cord injury. Eur. Spine J. 18, 1442–1451.
30. Detloff, M.R., Fisher, L.C., Deibert, R.J., and Basso, D.M. (2012). Acute and chronic tactile sensory testing after spinal cord injury in rats. J. Vis. Exp. e3247.
31. Bresnahan, J.C., Beattie, M.S., Stokes, B.T., and Conway, K.M. (1991). Three-dimensional computer-assisted analysis of graded contusion lesions in the spinal cord of the rat. J. Neurotrauma 8, 91–101.
32. Poon, P.C., Gupta, D., Shoichet, M.S., and Tator, C.H. (2007). Clip compression model is useful for thoracic spinal cord injuries: histologic and functional correlates. Spine 32, 2853–2859.
33. Hughes, J.T. (1984). Regeneration in the human spinal cord: a review of the response to injury of the various constituents of the human spinal cord. Paraplegia 22, 131–137.
34. Piani, D., Frei, K., Do, K.Q., Cuenod, M., and Fontana, A. (1991). Murine brain macrophages induced NMDA receptor mediated neurotoxicity in vitro by secreting glutamate. Neurosci. Lett. 133, 159–162.
35. Chao, C.C., Hu, S., Molitor, T.W., Shaskan, E.G., and Peterson, P.K. (1992). Activated microglia mediate neuronal cell injury via a nitric oxide mechanism. J. Immunol. 149, 2736–2741.
36. Tikka, T.M., and Koistinaho, J.E. (2001). Minocycline provides neuroprotection against N-methyl-D-aspartate neurotoxicity by inhibiting microglia. J. Immunol. 166, 7527–7533.
37. David, S., and Kroner, A. (2011). Repertoire of microglial and macrophage responses after spinal cord injury. Nat. Rev. Neurosci. 12, 388–399.
38. Schwab, J.M., Frei, E., Klusman, I., Schnell, L., Schwab, M.E., and Schluesener, H.J. (2001). AIF-1 expression defines a proliferating and alert microglial/macrophage phenotype following spinal cord injury in rats. J. Neuroimmunol. 119, 214–222.
39. Faden, A.I., Jacobs, T.P., and Helke, C.J. (1985). Changes in substance P and somatostatin in the spinal cord after traumatic spinal injury in the rat. Neuropeptides 6, 215–225.
40. Sharma, H.S., Nyberg, F., Olsson, Y., and Dey, P.K. (1990). Alteration of substance P after trauma to the spinal cord: an experimental study in the rat. Neuroscience 38, 205–212.
41. Rybarova, S., Kluchova, D., Schmidtova, K., and Kocisova, M. (1999). The influence of transient spinal ischemia on substance P positive nerve structures. Gen. Physiol. Biophys. 18, Suppl 1, 75–77.
42. O'Connor, T.M., O'Connell, J., O'Brien, D.I., Goode, T., Bredin, C.P., and Shanahan, F. (2004). The role of substance P in inflammatory disease. J. Cell Physiol. 201, 167–180.
43. Nakaya, Y., Kaneko, T., Shigemoto, R., Nakanishi, S., and Mizuno, N. (1994). Immunohistochemical localization of substance P receptor in the central nervous system of the adult rat. J. Comp. Neurol. 347, 249–274.
44. Vita, G., Haun, C.K., Hawkins, E.F., and Engel, W.K. (1990). Effects of experimental spinal cord transection on substance P receptors: a quantitative autoradiography study. Neuropeptides 17, 147–153.
45. Woie, K., Koller, M.E., Heyeraas, K.J., and Reed, R.K. (1993). Neurogenic inflammation in rat trachea is accompanied by increased negativity of interstitial fluid pressure. Circ. Res. 73, 839–845.
46. Tian, D.S., Liu, J.L., Xie, M.J., Zhan, Y., Qu, W.S., Yu, Z.Y., Tang, Z.P., Pan, D.J., and Wang, W. (2009). Tamoxifen attenuates inflammatory-mediated damage and improves functional outcome after spinal cord injury in rats. J. Neurochem. 109, 1658–1667.
47. Austin, J.W., Afshar, M., and Fehlings, M.G. (2012). The relationship between localized subarachnoid inflammation and parenchymal pathophysiology after spinal cord injury. J. Neurotrauma 29, 1838–1849.
48. Noble, L.J., and Wrathall, J.R. (1987). The blood-spinal cord barrier after injury: pattern of vascular events proximal and distal to a transection in the rat. Brain Res. 424, 177–188.
49. Jaeger, C.B., and Blight, A.R. (1997). Spinal cord compression injury in guinea pigs: structural changes of endothelium and its perivascular cell associations after blood-brain barrier breakdown and repair. Exp. Neurol. 144, 381–399.
50. Schwartz, E.D. (2005). MRI and the evaluation of the blood-spinal cord barrier following injury. AJNR Am. J. Neuroradiol. 26, 1609–1610.
51. Pan, W., Kastin, A.J., Bell, R.L., and Olson, R.D. (1999). Upregulation of tumor necrosis factor alpha transport across the blood-brain barrier after acute compressive spinal cord injury. J. Neurosci. 19, 3649–3655.
52. Popovich, P.G., Horner, P.J., Mullin, B.B., and Stokes, B.T. (1996). A quantitative spatial analysis of the blood-spinal cord barrier. I. Permeability changes after experimental spinal contusion injury. Exp. Neurol. 142, 258–275.
53. Griffiths, I.R. (1975). Vasogenic edema following acute and chronic spinal cord compression in the dog. J. Neurosurg. 42, 155–165.
54. Papadopoulos, M.C., Manley, G.T., Krishna, S., and Verkman, A.S. (2004). Aquaporin-4 facilitates reabsorption of excess fluid in vasogenic brain edema. FASEB J 18, 1291–1293.
55. Kimura, A., Hsu, M., Seldin, M., Verkman, A.S., Scharfman, H.E., and Binder, D.K. (2010). Protective role of aquaporin-4 water channels after contusion spinal cord injury. Ann. Neurol. 67, 794–801.
56. Mao, L., Wang, H.D., Pan, H., and Qiao, L. (2011). Sulphoraphane enhances aquaporin-4 expression and decreases spinal cord oedema following spinal cord injury. Brain Inj. 25, 300–306.
57. Sypert, G.W. (1990). Thoracolumbar fusion techniques. Clin. Neurosurg. 36, 186–216.
58. Horn, E.M., Theodore, N., Assina, R., Spetzler, R.F., Sonntag, V.K., and Preul, M.C. (2008). The effects of intrathecal hypotension on tissue perfusion and pathophysiological outcome after acute spinal cord injury. Neurosurg. Focus 25, E12.
59. Batchelor, P.E., Kerr, N.F., Gatt, A.M., Cox, S.F., Ghasem-Zadeh, A., Wills, T.E., Sidon, T.K., and Howells, D.W. (2011). Intracanal pressure in compressive spinal cord injury: reduction with hypothermia. J. Neurotrauma 28, 809–820.

Address correspondence to:
Anna V. Leonard, PhD
School of Medical Sciences
Level 4 Medical School South
The University of Adelaide
Frome Road
Adelaide 5005
Australia

E-mail: anna.leonard@adelaide.edu.au